Self-Focusing and Raman Scattering of Laser Pulses in Tenuous Plasmas

T. M. Antonsen, Jr.,[a] and P. Mora
Centre de Physique Théorique, Ecole Polytechnique, 91128 Palaiseau, France
(Received 26 May 1992)

The propagation of laser pulses of intensity which is large enough for relativistic self-focusing to occur is strongly affected by Raman instabilities. Both large and small angle scattering are important. The latter is the most severe since it couples with relativistic self-focusing leading the pulses to acquire significant axial and transverse structure in a time of the order of the self-focusing time. This prevents smooth self-focused pulses propagation for distances longer than the Rayleigh length except for pulse duration of the order of the plasma period.

PACS numbers: 52.40.Db, 42.65.Jx, 52.35.Mw, 52.40.Nk

Recent technological advances of high intensities (of the order of 10^{18} W/cm^2), short pulses lasers (1 psec or less) [1] have revived the interest for relativistic self-focusing effects in plasmas [2–5]. This Letter shows that self-channeled pulses are subject to severe instabilities of the Raman [6] type which quickly erode the tail of the pulse, an effect even faster than the front erosion of the pulse described by Sprangle, Esarey, and Ting [5].

We consider situations where the pulse length τ is smaller than the inverse of the ion plasma frequency ω_{pi}, so that the motion of the ions can be neglected. For sufficiently large laser power, the relativistic corrections to the electron response to the wave field lower the effective plasma frequency thereby increasing the refractive index. In addition, the ponderomotive force tends to expell the electrons from the laser channel, usually enhancing the relativistic effect. Such self-focusing occurs when the laser beam power P is above a critical power [3,4] $P_L = 16.2(\omega/\omega_p)^2(10^9\ \mathrm{W})$, where $\omega_p = (4\pi q^2 n_0/m)^{1/2}$ is the plasma frequency based on the ambient density n_0, and q and m are the charge and mass of an electron. If the laser pulse duration is much longer than the plasma period, time-independent solutions can be found where the electrons are in equilibrium, the radial ponderomotive force being balanced by the electrostatic force due to charge separation [4]. If the laser pulse duration is comparable with the plasma period, the dynamics of the electrons has to be taken into account [5]. As a result, the degree of guiding varies along the pulse. In particular, the forward ponderomotive force pushes the electrons at the front of the pulse leading to an increase of the electron density and this effect tends to exactly cancel the relativistic effect. The front of the pulse then diffracts as a low intensity beam [5]. By using a two-dimensional analysis, we show in this Letter that the dynamics of the electrons is of fundamental importance even if the laser pulse duration is much longer than the plasma period, and that it is at the origin of the instabilities which erode the tail of the pulse. We find that it will be difficult to propagate smooth self-focused pulses through tenuous plasmas for distances longer than the Rayleigh length (the natural diffraction length), except for pulse duration of the order of the plasma period.

In order to investigate self-focusing of a finite duration pulse the paraxial and quasistatic [5] approximations are made. The paraxial approximation consists of writing the normalized radiation vector potential, $\hat{\mathbf{a}}(\mathbf{x},t) = q\mathbf{A}/mc^2$, where c is the speed of light, as a plane wave propagating in the z direction modulated by a slowly varying three-dimensional envelope

$$\hat{\mathbf{a}}(\mathbf{x},t) = \mathbf{a}(\mathbf{x}_\perp,\xi,t)\exp[i(k_0 z - \omega_0 t)] + \text{c.c.}, \tag{1}$$

where $\omega_0^2 = \omega_p^2 + k_0^2 c^2$, and where $\xi = c_g t - z$ measures distance back from the head of the radiation pulse which is moving with a group velocity $c_g = k_0 c^2/\omega_0$ in the positive z direction. This results in

$$\left(2i\frac{\omega_0}{c^2}\frac{\partial}{\partial t} + \nabla_\perp^2\right)\mathbf{a} = k_p^2\left(\frac{\delta n}{n_0} - \mathbf{a}\cdot\mathbf{a}^*\right)\mathbf{a}, \tag{2}$$

where we have dropped terms which are of order ω_p^2/ω_0^2 which are presumed to be small. The terms on the right-hand side represent the response of the plasma, whose density can be written as the sum of the ambient value, n_0, and a small perturbation δn. The term $\mathbf{a}\cdot\mathbf{a}^*$ represents the contribution of the first correction to the relativistic factor $\gamma = 1/(1 - v^2/c^2)^{1/2}$, where $\mathbf{v} = c\hat{\mathbf{a}}/\gamma$ is the jitter velocity of an electron in the radiation field, averaged over the period of time associated with the frequency of the radiation. Finally, the constant $k_p = \omega_p/c$ represents the plasma wave number.

The density perturbation appearing in Eq. (2) results from the forced excitation of a plasma wave disturbance by the ponderomotive potential of the radiation. The quasistatic approximation consists of assuming that the radiation envelope described by (2) changes little during the time which a plasma electron is within the envelope, resulting in

$$\left(\frac{\partial^2}{\partial\xi^2} + k_p^2\right)\frac{\delta n}{n_0} = \nabla^2(\mathbf{a}\cdot\mathbf{a}^*), \tag{3}$$

where we have used the fact that in the weakly relativistic limit the density response is linear in the ponderomotive potential, and where it has been assumed that the plasma

is a cold fluid.

We now outline the derivation of the dispersion relation which determines the stability of an infinite homogeneous pump as described by Eqs. (2) and (3). Using known techniques [7] this dispersion relation then gives information on the space-time evolution of disturbances in a finite-size laser pulse. The radiation field will be assumed to be plane polarized and consists of a pump of amplitude a_0 and two daughter waves a_+ and a_- propagating at an angle to the pump,

$$\mathbf{a}(\mathbf{x},\xi,t)=\mathbf{e}_p\{a_0+a_+\exp(i\phi)+a_-\exp(-i\phi^*)\}+\text{c.c.}, \tag{4}$$

where $\phi=\mathbf{k}_\perp\cdot\mathbf{x}_\perp+k_z\xi-\omega t$, $\mathbf{e}_p$ is a unit vector giving the direction of polarization, $\mathbf{k}$ and ω are the wave number and frequency shift of the scattered radiation, and $\mathbf{e}_p\cdot\mathbf{k}=\mathbf{e}_p\cdot\mathbf{e}_z=0$. The beating of the pump and scattered waves gives rise to a time- and space-dependent ponderomotive potential, which in turn drives an electron density perturbation of the form $\delta n/n_0=\eta\exp(i\phi)+\text{c.c.}$ Inserting the preceding expressions for the dependent variables into Eqs. (2) and (3), and combining the equations results in the dispersion relation, $D(\omega,\mathbf{k})=0$, where

$$D(\omega,\mathbf{k})=\left[\frac{2\omega\omega_0}{c^2}\right]^2-k_\perp^4-2k_\perp^2\frac{a_0^2k_p^2(k_p^2+k_\perp^2)}{k_z^2-k_p^2}. \tag{5}$$

This dispersion relation describes both the relativistic self-focusing instability as well as the near-forward Raman instability when both the Stokes and anti-Stokes scattered waves are taken into account [8]. Two different regimes of instability, corresponding to large and small scattering angles, are found to be important. Large angle scattering corresponds to the limit $k_\perp^2\gg k_p^2$. In a more complete paper [9], it is shown that this instability is convective and depends on the source or seed signal which is to be amplified. The amount of exponentiation, Γ, a disturbance experiences before it leaves the region of the pump increases with transverse wave number [for example, $\Gamma=(a_0^2k_pLk_\perp W)^{1/2}$ in the Raman regime [9] where W and L are the width and length of the laser pulse] and, thus, a cutoff has to be imposed on the solutions of Eqs. (2) and (3) to prevent unphysical behavior. Indeed the paraxial approximation leading to Eq. (2) is not valid when the scattering angle approaches 90°, as it does when the dynamics of the electrons are included. If the amount of amplification is large enough, a significant fraction of the radiation in the pulse can be scattered. This effect will be illustrated in the numerical simulations to be presented farther on.

On the other hand, for disturbances whose transverse wavelength is longer than the plasma wavelength we may neglect $k_\perp^2$ compared with k_p^2 in the parentheses in the numerator of Eq. (5). We will focus here on this limit, which corresponds to near-forward scattering. We use the method of determination of the impulse response due to a localized disturbance at $\mathbf{x}=0$ and $t=0$, as described by Bers [7]. Specifically, we define $\omega'=\omega-\mathbf{k}\cdot\mathbf{v}$ and the shifted dispersion relation $D_v(\omega',\mathbf{k})=D(\omega'+\mathbf{k}\cdot\mathbf{v},\mathbf{k})$ and solve simultaneously the equations $D_v=0$ and $dD_v/d\mathbf{k}=0$. As the resulting instability is absolute, insofar as its propagation in the perpendicular direction is concerned, we set the perpendicular part of the velocity $\mathbf{v}$ equal to zero. The equation $dD_v/d\mathbf{k}_\perp=0$ determines the perpendicular component of the wave vector,

$$k_\perp^2=-a_0^2k_p^4/(k_z^2-k_p^2). \tag{6}$$

Inserting this relation into the dispersion relation (5) allows one to calculate the frequency ω,

$$\frac{2\omega\omega_0}{c^2}=i\sigma\frac{a_0^2k_p^4}{k_z^2-k_p^2}, \tag{7}$$

where $\sigma=\pm1$. Eliminating ω between (7) and the equation $dD_v/dk_z=0$ then determines the axial wave number

$$\frac{(k_z^2-k_p^2)^2}{k_z}=i\sigma\frac{a_0^2k_p^4c^2t}{\omega_0\xi}, \tag{8}$$

where we have replaced v_z by $-\xi/t$. The above has both a Raman ($|k_z-k_p|\ll k_p$) and a Compton limit ($|k_z-k_p|\gg k_p$). For fixed ξ, the Raman limit applies for early times, and the Compton limit applies for later times. The transition occurs at a critical time t_c which is given by

$$t_c=T_R\frac{2k_p\xi}{k_p^2R^2a_0^2},$$

where $T_R=\omega_0R^2/2c^2$ is the Rayleigh time for a pulse of width R, and $k_p^2R^2a_0^2$ is essentially the peak power in the pulse normalized to the critical value for self-focusing. For our simulations to be presented, the Raman regime result is relevant. To estimate the amount of exponentiation for the impulse response, we calculate

$$\text{Im}\{\omega' t\}=\text{Im}\{\omega t+k_z\xi\}=k_p\xi\,\text{Im}\left\{i\sigma\frac{k_p^2}{2(k_z^2-k_p^2)}\frac{t}{t_c}+\frac{k_z}{k_p}\right\}.$$

At the critical time, this is of the order of the length of the pulse measured in plasma wavelengths. For times less than the critical time we have from (8) $k_z=k_p[1+(i\sigma t/4t_c)^{1/2}]$. This gives the following estimate for the amount of exponentiation:

$$\text{Im}\{\omega' t\}=k_p\xi\left[\frac{t}{2t_c}\right]^{1/2}=\left[\frac{a_0^2k_p\xi\omega_p^2t}{2\omega_0}\right]^{1/2}. \tag{9}$$

Thus, long pulses, with $k_pL\gg1$, will eventually lose their smooth shape and develop transverse and axial structure. The amount of time required for this structure to appear can be estimated from the above by setting $\text{Im}\{\omega' t\}=1$ and solving for t, $t=4T_R/k_pLa_0^2k_p^2R^2$. Thus, for pulses at or above the threshold for self-focusing, and which are longer than a plasma wavelength, the structure will ap-

pear on the order of a Rayleigh time. Since, as shown by Sprangle, Esarey, and Ting [5], the pulse must be longer than a plasma period to self-focus at all, it will be very difficult to produce a smooth self-focused laser pulse.

We now describe the results of numerical simulations of the propagation of laser pulses through plasmas. The numerical scheme is widely described in Ref. [9]. The results of several simulations are shown in Fig. 1. The initial radiation pulse had the form

$$a(x,\xi,t=0)=a_0\sin(\pi\xi/L)\times\exp(-x^2/R^2)[1+\cos(\pi x/X_{\max})]/2\,, \tag{10}$$

where for the plots of Fig. 1 the relevant parameters are $a_0=0.32$, $k_pL=80$, $k_pR=16$, and $k_pX_{\max}=32$. The last factor in (10) insures that, initially, the vector potential and its radial derivative vanish at the boundary. This reduces the high k components that would be present if the initial vector potential were simply cut off at the boundary. Figure 1(a) shows the field intensity at time $t=0.35T_R$. One can see the development of the large angle scattered radiation on the trailing end of the pulse. The axial wavelength of the perturbations is equal to the plasma wavelength, and the radial wavelength is equal to the shortest value allowed by the grid. This radiation has grown from the high k components of the initial wave form which are present due to its finite radial extent. Figure 1(b) shows a continuation of the same simulation now at one-half the Rayleigh time. Several important features are visible. First, the body of the pulse has self-focused to a high degree. As predicted by Sprangle, Esarey, and Ting [5], the head of the pulse has not focused. The high perpendicular radial wave number scattered radiation is still visible at the very end of the pulse, but its magnitude has diminished slightly from that in Fig. 1(a). A new perturbation is seen to develop in the body of the pulse. The axial wavelength of the perturbation is, again, the plasma wavelength but the radial wavelength is larger than that of the perturbation at the tail of the pulse. Figure 1(c) shows the shape of the pulse at 2.0 Rayleigh times. The tail of the pulse has now been completely eroded by scattering. The degree of scattering is dramatic due to our choice of a rather large initial normalized field amplitude. Because of the relatively long radial wavelength of the scattered radiation in this case we interpret this instability as being the coupled Raman–self-focusing branch discussed previously. This scattering is an inherent feature of intense pulse propagation in tenuous plasmas. Figure 2 illustrates the degree of self-focusing present for a simulation with the parameters $a_0=0.16$, $k_pL=40$, $k_pR=20$, and $k_pX_{\max}=160$. Plotted is the rms width of the pulse as a function of axial distance for several different times. The body of the pulse remains focused for the duration of the simulation. There is, however, considerable excitation of the Raman instability as evidenced by the appearance of oscillations on the tail of the pulse with period equal to the plasma wavelength. The degree of self-focusing seen here is probably enhanced due to the fact that our simulation geometry is planar as opposed to cylindrical. In planar geometry the power density on axis in the head of the pulse decays with time as t^{-1} instead of t^{-2} as would be expected in cylindrical geometry. This is important for the self-focusing of the body of the pulse because the head of the pulse produces the modification of the index of refraction that focuses the body of the pulse. Thus, in cylindrical geometry one might see a faster erosion of the head of the pulse which eventually leads to a defocusing

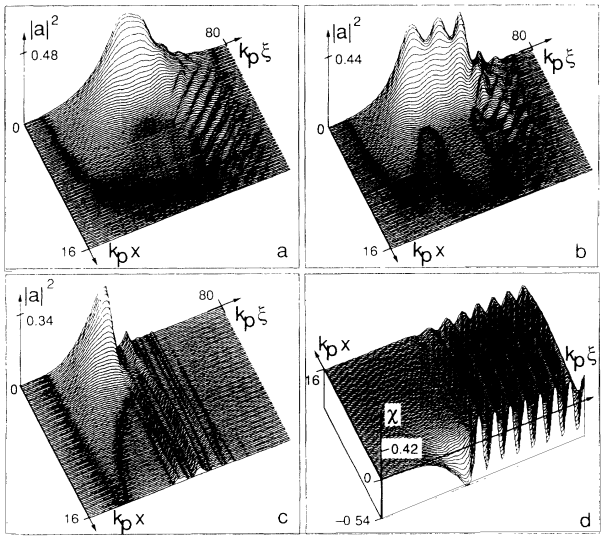

FIG. 1. (a)–(c) Normalized intensity and (d) perturbation of the index of refraction as function of space. On these three-dimensional plots the laser is propagating from the right to the left. The parameters correspond to $a_0=0.32$, $k_pL=80$, $k_pR=16$, and $k_pX_{\max}=32$. (a) $t=0.35T_R$, (b) $t=0.5T_R$, (c),(d) $t=2T_R$. Note that, for convenience, the x axis has been inverted on (d).

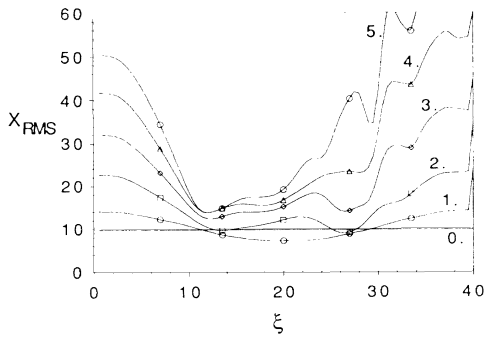

FIG. 2. Root-mean-squared width of the pulse as a function of the axial distance for $t=0$ to $5T_R$. Parameters are $a_0=0.16$, $k_pL=40$, $k_pR=20$, and $k_pX_{\max}=160$.

of the body. Finally, Fig. 1(d) shows the perturbation of the index of refraction, $\chi=(\delta n/n_0)-\mathbf{a}\cdot\mathbf{a}^*$, for the case of Fig. 1(c). The largest perturbations occur behind the pulse where, due to scattering, the field amplitude is very small. Thus, what is plotted here is essentially the density perturbation. The relative density perturbations are quite large in this case. Indeed, it was necessary in our simulations to restrict the range of the index of refraction to prevent the density from becoming negative. The restriction would not be necessary if the fully relativistic and electromagnetic equations [10] for the plasma response were calculated instead of the weakly relativistic equations used here.

In conclusion, we have examined the excitation of Raman instabilities as they affect the propagation of short pulses in tenuous plasmas. Two regimes of Raman instability, corresponding to relatively large and relatively small scattering angles, are important. For the large angle case, the instability is convective in the frame of the moving pulse, and the amount of amplification increases with scattering angle. The resulting plasma wake appears to be incoherent. However, the effect of this instability may be mitigated by the inclusion of nonlinear terms [10] in the plasma response. The small angle scattering instability is absolute in space, and results from a coupling of the Raman and self-focusing mechanisms. It causes the pulse to develop transverse and axial structure within a Rayleigh time. The resulting plasma wake appears to be coherent; however, its suitability for particle acceleration needs to be investigated. In all cases the instability becomes more severe as the length and intensity of the pulse is increased. Thus, due to these instabilities, stable pulse propagation over many Rayleigh lengths can only be expected for pulses which are not too long, $k_pL=10$–20. The trailing end of pulses which are longer than this limit will be side scattered until the pulse is shortened to a stable length. This effect, combined with the diffraction of the head of the pulse [5], severely limits the parameters for which effective self-focusing will occur.

We acknowledge fruitful discussions with D. Pesme. One of the authors (T.M.A.) would like to thank the Centre National de la Recherche Scientifique for its support and the members of the Centre de Physique Theorique of the Ecole Polytechnique for their hospitality.

[a]Permanent address: Department of Electrical Engineering and Department of Physics, University of Maryland, College Park, MD 20742.

[1] P. Maine *et al.*, IEEE J. Quantum Electron. **24**, 398 (1988).

[2] C. E. Max, J. Arons, and A. B. Langdon, Phys. Rev. Lett. **33**, 209 (1974).

[3] G. Schmidt and W. Horton, Comments Plasma Phys. Controlled Fusion **9**, 85 (1985).

[4] G. Z. Sun *et al.*, Phys. Fluids **30**, 526 (1987); W. B. Mori *et al.*, Phys. Rev. Lett. **60**, 1298 (1988); T. Kurki-Suonio, P. J. Morrison, and T. Tajima, Phys. Rev. A **40**, 3230 (1989); P. Gibbon, Phys. Fluids B **2**, 2196 (1990); A. B. Borisov *et al.*, Phys. Rev. Lett. **68**, 2309 (1992).

[5] P. Sprangle, E. Esarey, and A. Ting, Phys. Rev. Lett. **64**, 2011 (1990).

[6] J. F. Drake *et al.*, Phys. Fluids **17**, 778 (1974); W. M. Manheimer and E. Ott, Phys. Fluids **17**, 1413 (1974); R. Pellat, in *Laser-Plasma Interaction,* Proceedings of the Les Houches Summer School, Session XXXIV, edited by R. Balian and J. C. Adam (North-Holland, Amsterdam, 1982), p. 411; D. Pesme, Interaction Laser Matière 1986 Report, 1987 (unpublished), pp. 21–32; P. Sprangle and E. Esarey, Phys. Rev. Lett. **67**, 2021 (1991).

[7] A. Bers, in *Basic Plasma Physics I,* edited by A. A. Galeev and R. N. Sudan, Handbook of Plasma Physics Vol. 1, edited by M. N. Rosenbluth and R. Z. Sagdeev (North-Holland, New York, 1983), p. 451.

[8] Equation (5) can be obtained by applying the quasistatic and paraxial approximations to dispersion relation (5) of C. J. McKinstrie and R. Bingham, Phys. Fluids B **4**, 2626 (1992).

[9] T. M. Antonsen, Jr., and P. Mora (to be published).

[10] B. Breizman *et al.* (private communication).

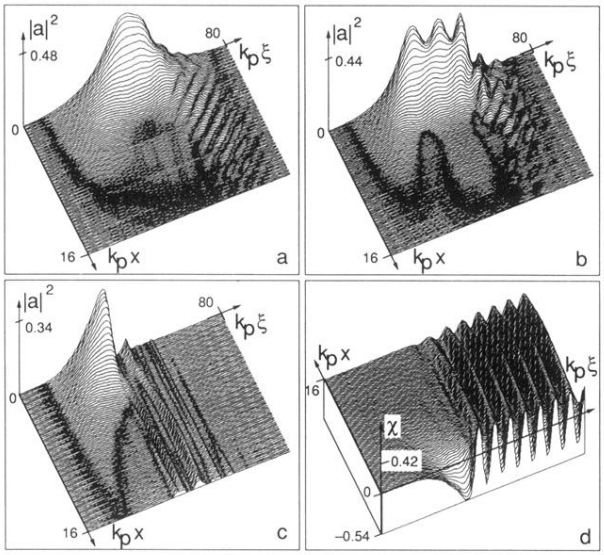

FIG. 1. (a)–(c) Normalized intensity and (d) perturbation of the index of refraction as function of space. On these three-dimensional plots the laser is propagating from the right to the left. The parameters correspond to $a_0=0.32$, $k_pL=80$, $k_pR=16$, and $k_pX_{\max}=32$. (a) $t=0.35T_R$, (b) $t=0.5T_R$, (c),(d) $t=2T_R$. Note that, for convenience, the x axis has been inverted on (d).